Ultralow-Energy Electrons from Fast Heavy-Ion Helium Collisions: The "Target Cusp"

W. Schmitt,[1,2] R. Moshammer,[1] F. S. C. O'Rourke,[3] H. Kollmus,[1] L. Sarkadi,[4] R. Mann,[2] S. Hagmann,[5] R. E. Olson,[6] and J. Ullrich[1,*]

[1]*Universität Freiburg, Hermann-Herder Strasse 3, D-79104 Freiburg, Germany*
[2]*Gesellschaft für Schwerionenforschung, D-64220 Darmstadt, Germany*
[3]*The Queen's University of Belfast, Belfast BT7 1NN, United Kingdom*
[4]*Institute of Nuclear Research of the Hungarian Academy of Sciences, POB 51, H-4001 Debrecen, Hungary*
[5]*J. R. MacDonald Laboratory, Kansas State University, Manhattan, Kansas 66506*
[6]*Department of Physics, University of Missouri-Rolla, Rolla, Missouri 65401*

(Received 8 April 1998)

Doubly differential cross sections $d^2\sigma/dv_\parallel dv_\perp$ have been obtained by mapping the 3-dimensional velocity space of ultralow- and low-energy electrons (1.5 meV $\leq E_e \leq$ 100 eV) emitted in singly ionizing 3.6 MeV/u Au^{53+} on helium collisions. A sharp ($\Delta E_{e\perp}^{\mathrm{FWHM}} \leq 22$ meV) asymmetric peak centered at $|\vec{v}| = 0$ is observed to emerge at ultralow energies from the strongly forward shifted low-energy electron velocity distribution. The shape of this "target cusp," which is very sensitive on the details of the two-center potential, is in excellent accord with theoretical predictions. [S0031-9007(98)07590-5]

PACS numbers: 34.10.+x, 34.50.Fa

Single ionization of a target atom is one of the dominant reaction channels in ion-atom collisions and therefore of basic importance for a large manifold of applications (implantation of ions in substrates, plasma heating, surface modifications, cancer therapy with heavy ions, etc.). Even more surprising, after about four decades of systematic electron spectroscopy in ion- and electron-atom collisions by many groups (for recent reviews see, e.g., [1,2]), there are only two data sets of doubly differential experimental cross sections $d^2\sigma/dE_e d\Omega$ for the emission of electrons with energies E_e below 1 eV. Two more studies are at hand extending down to $E_e \approx 1$ eV, and very few reliable data sets are available for $E_e < 10$ eV (using conventional spectrometers experimental uncertainties were estimated [2] to be as large as 30% for $E_e < 5$ eV and up to 50% for $E_e = 1$ eV). Other techniques developed to detect low-energy electrons [3] so far gave only access either to the total energy or to two velocity components without any energy information. Thus, in essence, low ($E_e < 10$ eV) and ultralow energy ($E_e \lesssim 1$ meV) continuum electrons in the (screened) Coulomb potential of the target or in the two-center potential of the target and projectile remained unexplored experimentally.

Basic questions on this fundamental three-particle process arise. According to the general Wigner threshold law for long-range interactions $d^2\sigma/dE_e d\Omega$ has a finite (nonzero) value at the threshold, i.e., at $v = 0$. From that it follows that the cross-section differential in the electron velocity $d\sigma/d|\vec{v}|$ diverges as $d\sigma/d|\vec{v}| \propto 1/v$. This divergence also emerges from calculations in the first Born approximation (FBA), and a symmetric angular distribution was predicted for hydrogenic targets in the limit of $v \to 0$ (see, e.g., [4]). Calculations beyond the FBA (see, e.g., [5]) expand low-lying continuum states in terms of high-lying Rydberg states. They predict distinct asymmetric angular distributions of the electrons depending on the velocity of the exciting particle, on the nodal structure of the initial state, as well as on the postcollision interaction between the electrons and the emerging projectile. Moreover, applying the continuum distorted wave approximation (CDW), it was shown [6] that the properties of the soft-electron emission for multielectron targets sensitively depend on the wave functions employed. Last but not least, nothing is known experimentally as well as theoretically on the three particle dynamics at the singularity where the final electron momentum is zero.

In order to reliably explore the low-energy electron emission, a resolution of $\Delta v_i = 9 \times 10^{-3}$ a.u. ($\Delta E_i =$ 1.1 meV) along all three dimensions in velocity space was theoretically estimated to be necessary [5]. This is in agreement with recent FBA and CDW results for 100 keV p on He collisions, indicating that the low-energy asymptotic limit for the angular distribution is reached at 10^{-4} eV (page 128 of Ref. [2]). This is far beyond the resolutions achieved in recent experiments when traditional techniques are used [7]. Nevertheless, the exploration of the "soft-electron peak" (SEP) has attracted increasing attention [8–13]. Studies concentrated on the investigation of its asymmetry along the forward-backward direction (early data; see, e.g., [9,14]).

Soft projectile-centered electrons produced either by excitation of a "clothed" projectile (electron loss to the continuum, ELC) or the capture of an electron into the projectile continuum (ECC) have been explored over more than two decades (see, e.g., [2]). In the laboratory frame these electrons show themselves as a sharp "cusplike" peak at an emission angle close to 0° and a velocity centered around the projectile velocity v_p. Unlike the "target cusp" the projectile cusp exists in both the velocity and energy spectrum due to the kinematic transformation. As a further consequence of transformation [4], the experimental

resolution in the projectile frame along v_p increases linearly with v_p, reaching values as good as $\Delta v_{e\parallel} = 10^{-2}$ a.u. at $v_p = 10$ a.u., whereas the transverse resolution decreases with v_p and is about a factor of 10 worse at the same velocity (see, e.g., [15]).

In this Letter we report on the measurement of ultralow energy electrons in the target frame, on the observation of the target cusp, i.e., the predicted singular behavior at $v = 0$ in the three-dimensional velocity space, and on the detailed investigation of its shape. Applying a rigorously new combined magnetic and electric projection technique for low-energy electron detection, we were able to increase the energy resolution of state-of-the-art conventional spectrometers by at least 2 orders of magnitude in each dimension of the velocity space to $\Delta E_{ei} = 2.5$ meV for $\vec{v} \rightarrow 0$.

The experiments were performed with a substantially improved version of our "reaction microscope" using a tightly collimated charge-state analyzed 3.6 MeV/u Au^{53+} beam from the UNILAC (Universal Accelerator) of GSI (Gesellschaft für Schwerionenforschung). Working principle, design, and resolution of the microscope have been described in detail before [16,17]. In short, low-energy ions and electrons emerging from a 2.8 mm diam supersonic jet are accelerated into opposite directions by a 1.36 V/cm electric field applied along the ion beam (longitudinal direction). The transverse motion of the electrons is confined by an additional solenoidal magnetic field of 6.1 G ($\Delta B/B = 8 \times 10^{-4}$) for the high resolution measurements (20.5 Gauß for lower resolution). In this way all electrons with transverse energies below 10 eV (115 eV) and longitudinal energies below 15 eV are projected on a 75 mm diam two-dimensional position sensitive microchannel plate detector placed 33 cm downstream the jet target ("time focusing geometry," see [17]). From the measured absolute positions and flight times, the ion and electron trajectories are reconstructed and their initial momenta are calculated. For the electrons, the achieved time resolution of 1 ns resulted in a longitudinal velocity resolution of $\Delta v_{\parallel} = 1 \times 10^{-2}$ a.u. (total time of flight for $v_{\parallel} = 0$ is 203 ns). A position resolution of $\Delta x, y = 0.6$ mm (ion beam diameter) gave an optimum transverse velocity resolution of $\Delta v_{\perp}^{\mathrm{opt}} = 1.4 \times 10^{-2}$ a.u. when the electron is at its maximum distance (35 mm) from the target point on the course of its cyclotron motion (time for a complete turn, 58.6 ns). The fields were adjusted in such a way that the optimum resolution was exactly reached for electrons with $v = 0$ a.u. Extreme care has been taken and various methods were applied and compared (trajectory calculations, extrapolation from the cyclotron frequency, retarding fields) for the calibration of the velocity axis in both directions, and an accuracy of ± 0.005 a.u. has been obtained, respectively.

Our technology provides several new features: (1) The full kinematics for single ionization (nine-dimensional velocity space) is determined for defined final charge state of projectile and target. Thus, the inelasticity of the reaction is inherently measured and the final electronic states of the projectile and the target are controlled. (2) Any differential cross section (projected from the 9-dimensional space) can be brought on an absolute scale. A short run at a sufficiently high magnetic and electric field is normalized on the total single ionization cross section σ^{1+}. The present σ^{1+} is accurate within $\pm 20\%$ [18]. The accuracy of any projections (i.e., various differential cross sections) relative to each other is limited only by the statistical errors. (3) All electrons emitted into the 4π solid angle with velocities below the given acceptance are detected, including those with $v = 0$, the notoriously critical point of conventional devices. (4) Triple coincidence spectra are free from background on the level of 3 orders of magnitude; contributions from the rest gas are completely absent.

In Fig. 1 the experimental longitudinal velocity distributions for different transverse velocities; i.e., doubly differential cross sections (DDCS) are shown in comparison with results of CDW eikonal-initial-state (CDW-EIS) calculations (lines). This represents the up-to-date most complete experimental map of the soft-electron peak for $E_{e\parallel} < 127$ eV and $E_{e\perp} < 13.6$ eV including $E_e = 0$. Cylindrical coordinates in velocity space with the axis along the beam propagation are well adapted to the azimuthal symmetry of the electron emission if no scattering plane is

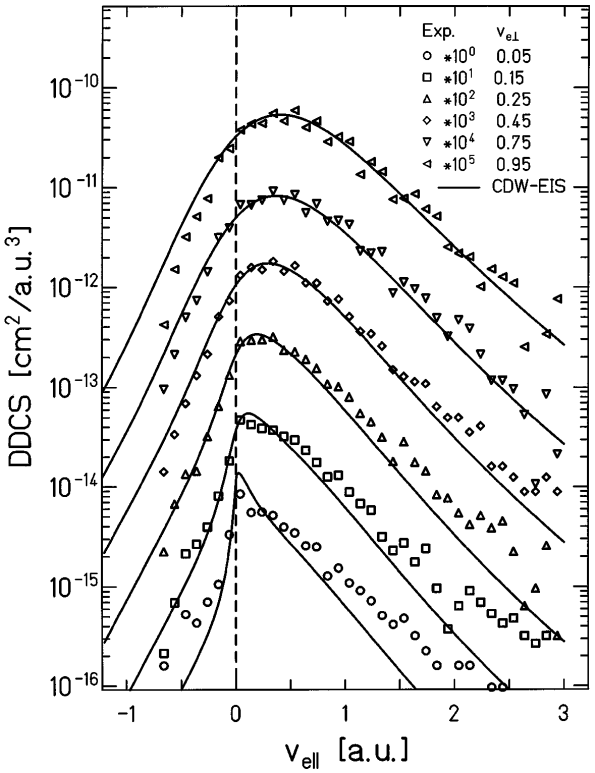

FIG. 1. Doubly differential cross sections DDCS $= d^2\sigma/(dv_{\parallel}dv_{\perp} \cdot 2\pi v_{\perp})$ as a function of the longitudinal electron velocity (see text) for various transverse velocity cuts in singly ionizing 3.6 MeV/u Au^{53+} on He collisions. Cross sections at different $v_{\perp}$ are multiplied by factors of 10, respectively. Lines: theoretical CDW-EIS results.

defined. They are commonly used for the representation of ELC or ECC electrons. The presented DDCS are defined as DDCS $= d^2\sigma/[dv_\parallel dv_\perp(2\pi v_\perp)]$ in order to correct for the increasing volume element with increasing $v_\perp$. Thus, they have the shape and dimension of triply differential cross sections $d\sigma/d\vec{v}$ assuming azimuthal symmetry.

Excellent agreement between theory and experiment is observed in shape as well as in absolute magnitude. A strong forward-backward asymmetry is found. The whole distributions including their maxima for the larger transverse momenta are shifted towards positive velocities. This asymmetry has been observed before in $d^2\sigma/dE_e d\Omega$ at higher electron energies (see [2] and references therein) as well as in singly differential cross sections $d\sigma/dv_\parallel$, and it was attributed to the postcollision interaction (PCI, in literature often used as a synonym for two-center effects). The emerging highly charged projectile providing a large perturbation strength of $q/v_p = 4.4$ (q and v_p are the projectile charge and velocity, respectively) pulls the electron into the forward direction.

In Fig. 2 the shape of the DDCS (at $v_\perp = 0.75$ a.u.) as a function of $v_\parallel$ is compared to the results of a CDW-EIS calculation at a tiny perturbation of $q/v_p = 0.04$ (normalized to the same $d\sigma/dv_\perp$) where two-center effects essentially should be absent. At large $q/v_p =$ 4.4 the emission of low-energy electrons ($E_e < 5$ eV) is strongly suppressed by nearly a factor of 10 in the backward direction due to PCI, whereas forward emission is strongly enhanced.

Proceeding to smaller and smaller transverse velocities, the DDCS strongly increase at $v_{e\parallel} = 0$, illustrating the increasing influence of the target charge onto the electron emission characteristics for tiny $v_\perp$. In Fig. 3 a sharp cusp-shaped peak is observed centered at $v_\parallel = 0$ for a transverse velocity cut of $\Delta v_\perp \leq 0.04$ a.u. Still, this target cusp of ultralow energy electrons is found to be strongly asymmetric due to PCI in excellent accord with results of classical trajectory Monte Carlo calculations (CTMC) as well as CDW-EIS results (see, e.g., [19]). Because of the statistical fluctuations of the data in this small volume of velocity space, the present experiment cannot distinguish between both theories which differ in the prediction of the shape by up to 35%. CDW-EIS calculations for energies as low as 10 μeV predict the target cusp to remain asymmetric raising the questions as what will happen in the limit of $\vec{v} \to 0$ beyond the present resolution. At very low energies the calculated shape of the target cusp is systematically in better agreement with experiment than at higher electron energies (see the discussion in [10]). For larger transverse velocities of up to 0.25 a.u. (see three lower data sets in Fig. 1) the asymmetry is underestimated for $v_{e\parallel} \geq 1$ a.u. which is in qualitative agreement with the previous findings [10].

Inspection of the target cusp along the transverse direction (Fig. 4) yields an even steeper rise and proves the singular behavior of the ultralow energy electron emission within the present resolution. The longitudinal velocity cut of $\Delta v_\parallel < \pm 5 \times 10^{-3}$ a.u. corresponds to the estimated upper limit of the longitudinal energy resolution of $\Delta E_{e\parallel} < \pm 350$ μeV. The transverse direction is found to be less affected by the influence of two-center effects and displays a $(1/v_\perp)$ behavior (full line) within the error

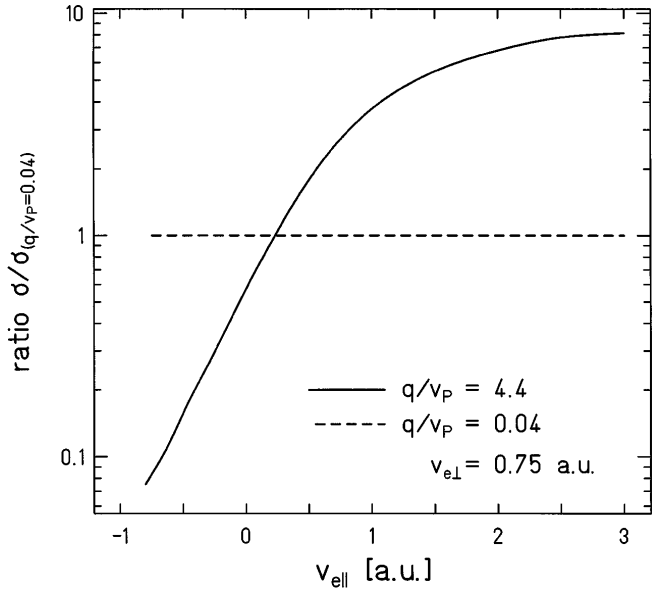

FIG. 2. Doubly differential CDW-EIS cross section $d^2\sigma/dv_\parallel dv_\perp$ at $v_\perp = 0.75$ a.u. for $q/v_p = 4.4$ divided by CDW-EIS results for $q/v_p = 0.04$ for the above collision system normalized on the same $d\sigma/dv_\perp$.

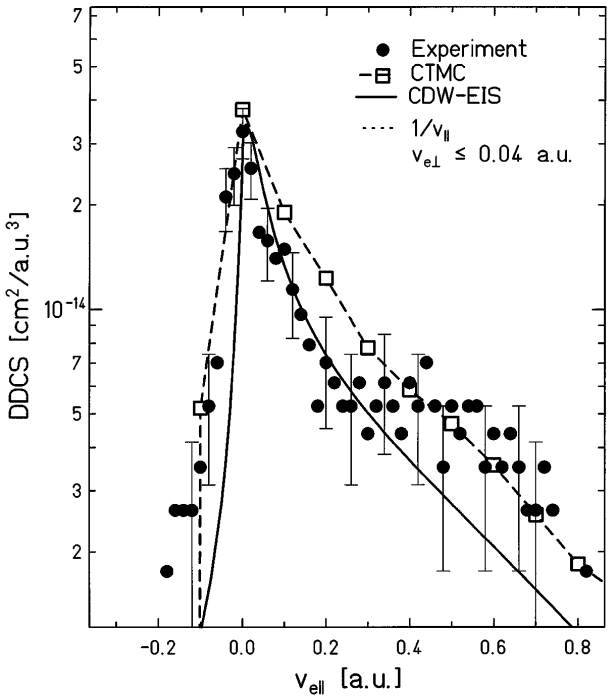

FIG. 3. Same as Fig. 1 for a transverse velocity cut of $v_\perp \leq$ 0.04 a.u. Dashed line: theoretical CTMC results. Full line: CDW-EIS results.

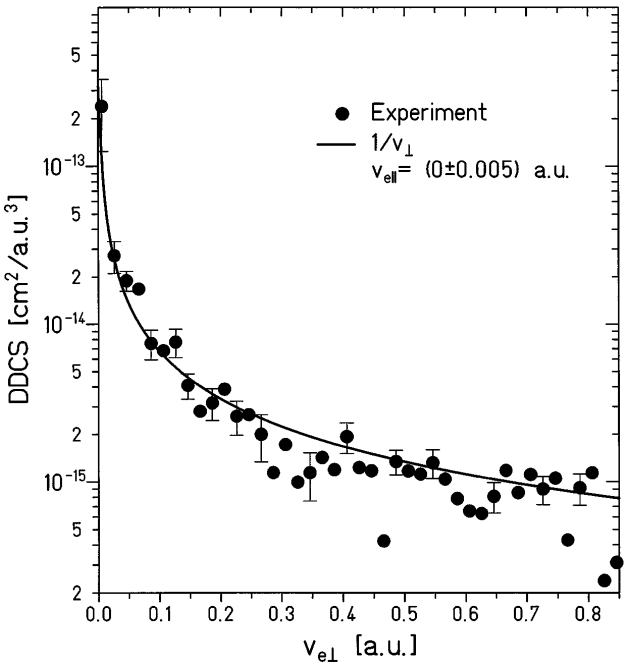

FIG. 4. Doubly differential cross section DDCS $= d^2\sigma/(dv_\parallel dv_\perp \cdot 2\pi v_\perp)$ as a function of the transverse velocity (see text) for the indicated longitudinal velocity cut. Full line: $1/v_\perp$ behavior.

bars. Our experiments were strongly motivated by the question of whether or not and down to what energy the cusp might exist. Obviously, for $E_e = 0$, electrons will stay infinitely long in the continuum of their parent ion and will definitely recombine due to the coupling to the radiation field (see, e.g., the investigation of radiative recombination in cooler sections of storage rings). In other words, at $v = 0$ the target cusp should disappear and, consequently, its shape will be strongly modified at velocities even lower than those investigated here.

In summary, using a substantially improved reaction microscope, the emission characteristics of low- to ultra-low energy target electrons was explored with unprecedented precision. The existence of the target cusp was established down to energies of a few meV. Strong two-center effects were observed over the whole range of electron energies investigated, even at a few meV, in excellent accord with CTMC and CDW-EIS predictions. CDW-EIS calculations reproduce the data in the whole range investigated on a remarkable level. For emission into the forward direction ($v_\perp \leq 0.25$ a.u.), the CDW-EIS calculations were found to underestimate the asymmetry unless one goes to very small $v_\perp \leq 0.04$ a.u., where agreement is found within the experimental error bars.

In the future, the three particle dynamics for the target cusp electron production will be explored. One major goal will be the investigation of the coupling to the radiation field. Providing laser to microwave fields, transitions from the continuum into bound states are induced, "burning trenches" into the cusp. Using state prepared Li or Na targets, predicted structures like an "anticusp" formation for aligned $m = 0$ states should become observable [20]. Furthermore, the calculated dependence of the cross sections on the initial state wave function of multielectron targets ([6], Fig. 5.13 in [2]) will become accessible.

Support from GSI and from the Deutsche Forschungsgemeinschaft within the SFB 276, project B8, is gratefully acknowledged. One of us (L. S.) would like to thank the DAAD, supporting the visit at GSI. We want to thank the GSI accelerator crew for providing an excellent beam and A. Bardonner for mechanical help.

*Email address: Ullrichj@uni-freiburg.de

[1] M. E. Rudd, Y.-K. Kim, D. H. Madison, and T. J. Gay, Rev. Mod. Phys. **64**, 441 (1992).
[2] N. Stolterfoht, R. D. DuBois, and R. D. Rivarola, *Electron Emission in Heavy-Ion Atom Collisions*, edited by J. P. Toennies (Springer-Verlag, Berlin, 1997), Vol. 20.
[3] R. Dörner *et al.*, Phys. Rev. Lett. **77**, 4520 (1996); S. D. Kravis *et al.*, Phys. Rev. A **54**, 1394 (1996); M. Pieksma *et al.*, Phys. Rev. Lett. **73**, 46 (1994).
[4] M. Inokuti, Rev. Mod. Phys. **43**, 297 (1971); S. T. Manson *et al.*, Phys. Rev. A **12**, 60, (1975); F. Drepper and J. Briggs, J. Phys. B. **9**, 2063 (1976).
[5] J. Burgdörfer *et al.*, Phys. Rev. A **28**, 3277 (1983).
[6] P. D. Fainstein *et al.*, Phys. Rev. A **53**, 3243 (1996).
[7] S. Suárez *et al.*, Phys. Rev. A **48**, 4339 (1993).
[8] S. Suárez *et al.*, Phys. Rev. Lett. **70**, 418 (1993).
[9] N. Stolterfoht *et al.*, Phys. Rev. A **52**, 3796 (1995).
[10] F. D. Colavecchia, W. Cravero, and C. R. Garibotti, Phys. Rev. A **52**, 3737 (1995).
[11] G. W. Kerby III *et al.*, Phys. Rev. A **51**, 2256 (1995).
[12] L. Tribedi *et al.*, Phys. Rev. A **54**, 2154 (1996).
[13] R. Moshammer *et al.*, Phys. Rev. Lett. **73**, 3371 (1994).
[14] M. E. Rudd and T. Jorgensen, Jr., Phys. Rev. **131**, 666 (1963).
[15] W. Meckbach, I. B. Nemirovsky, and C. R. Garibotti, Phys. Rev. A **24**, 1793 (1981).
[16] R. Moshammer *et al.*, Nucl. Instrum. Methods B **108**, 425 (1996).
[17] H. Kollmus *et al.*, Nucl. Instrum. Methods B **124**, 377 (1997).
[18] H. Berg *et al.*, J. Phys. B **25**, 3655 (1992).
[19] S. F. O'Rourke, R. Moshammer, and J. Ullrich, J. Phys. B **30**, 5281 (1997).
[20] Gulyás *et al.*, Phys. Rev. A **45**, 4535 (1992).